Jet scour

by Gijs Hoffmans[1] and Henk Verheij[2]

This paper discusses scour without bed protection, such as propeller scour, 2D-H (= two-dimensional horizontal), 3D-H scour generated by free jets downstream of gates and outlets, 2D-V (= two-dimensional vertical) and 3D-V scour. The flow velocities in 2D and 3D propeller and free jets are briefly summarized where special attention is paid to the Dutch and German approaches for calculating the near-bed load caused by propellers. The time scale of propeller scour is approximated by applying the Breusers' time-dependent scour equation. For the maximum scour depth in the equilibrium phase Newton's second law is used.

1 Jet types and hydraulic phenomena

In general, the following 2D and/or 3D jet forms can be considered

- downstream of hydraulic structures
- equalizing water levels in locks
- spillways
- downstream of spurs in a river
- diffusors (very often multiple jets)
- propeller jets of ships

Horizontal 2D flows are considered flows under barriers or gates which are infinitely, i.e. sufficiently wide (Fig. 1). Underflow has a considerable potential for scour caused by either high flow velocities or high turbulence intensities. Following Schoklitsch (1935, 1962) it is possible to distinguish attached jets (or wave or plunging jumps) and surface jets (or moving or inverted jumps) in which the jet form depends on a number of factors such as submergence, flow and turbulence patterns.

Attached jets (or wall jets) are characterised by a combination of high near-bed velocities and low-bed turbulence. Surface jets are symbolised by two different flow velocities occurring in the undisturbed flow and the deceleration or recirculation zone where the near-bed velocities are relatively small. At the interface, which is in the mixing layer where the velocity gradients and the turbulence intensities are at maximum, the flow is unstable.

Basic features of jets are: diffusion, mixing layers and the extra turbulence due to the decreasing flow velocities. All these phenomena are strongly related. For example, the generation of a mixing layer occurs between two adjacent streams that move at different speeds in the same general direction. Such a surface of discontinuity in the flow is unstable if the Reynolds number is large enough and gives rise to a zone of turbulent mixing downstream of the point where the two streams meet. The width of this mixing layer increases in the downstream direction.

The jet flow can be divided into two distinct regions (Albertson et al. 1948), namely a potential core and a diffused jet. The potential core is a wedge-like region in which the flow velocity equals the efflux velocity, whereas in the diffused jet the flow velocities decrease.

2 Hydraulic modelling

Theory assumes that the jet can be schematised as a submerged jet discharging out of an orifice into an infinite flow in which the jet velocities are Gaussian distributed around the axis. Directly downstream of a 2D-H outlet, the width of the mixing layer increases and the jet diffuses almost linearly. In a 2D-H diffused jet, the maximum time-averaged flow velocity ($\bar{u}_m$) decreases as (Albertson et al. 1948)

$$\bar{u}_m = (2\alpha_1)^{-1} U_e (b_u / x)^{\alpha_2} \tag{1}$$

in which b_u is the width of the 2D jet, U_e is the mean efflux velocity, x is the horizontal distance from the 2D outlet and α_1 (= 0.2) and α_2 (= 0.5) are coefficients

[1] Deltares, Delft, the Netherlands
[2] TU Delft and Deltares, Delft, the Netherlands

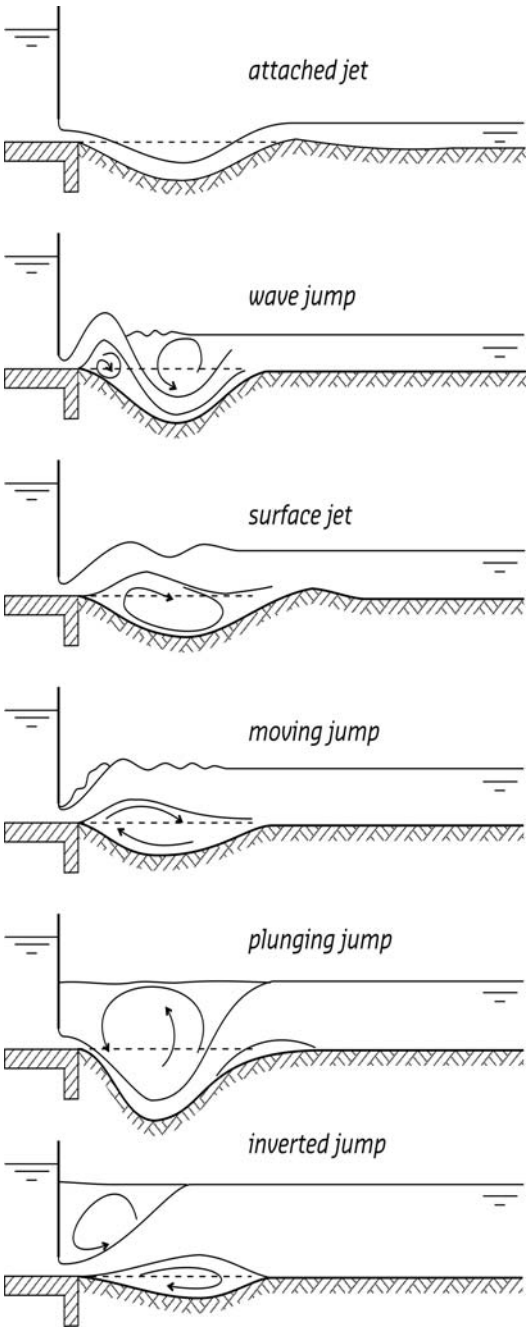

Fig. 1 Different jet forms (Schoklitsch 1935)

Jets, which are initiated by a propeller, accelerate flow in axial, radial and tangential directions. The flow behind a ship's propeller is comparable to a flow in a free (or 3D) jet, because in both flows the jet diffuses. However, there are also differences. The flow in a propeller jet diverges faster and the rotation and whirl in a propeller jet is higher, resulting in different patterns for flow and turbulence (Figs. 2 and 3). Following Albertson et al. (1948) the local jet velocity ($\bar{u}_{r,x}$) is in a 3D diffused jet (Fig. 4)

$$\bar{u}_{r,x} = \bar{u}_m \exp\left(-\frac{1}{2\alpha_1^2}\frac{r^2}{x^2}\right) \tag{2}$$

with

$$\bar{u}_m = (2\alpha_1)^{-1} U_e (D_p / x)^{\alpha_2} \tag{3}$$

where D_p is the 3D jet diameter (or propeller diameter) and r is the radial distance from the jet axis. The efflux velocity reads (Blaauw and Van de Kaa 1978)

$$U_e = 1.15\left(\frac{P}{\rho D_p^2}\right)^{1/3} \tag{4}$$

in which P is the installed engine power and ρ is the density of water.

The reattachment length of the jet (x_R) ranges from $4 < x_R / z_p < 10$ (e.g. Rajaratnam 1976), where z_p is the keel clearance. The maximum time-averaged near-bed velocity occurs at $x_R / z_p \approx 6$, giving

$$\bar{u}_{b,m} = \alpha_3 U_e (D_p / z_p) \tag{5}$$

in which $\alpha_3 = 0.2$. Fueher *et al*. (1981), Blaauw and Van de Kaa (1978) and Verheij (1983) use both Eqs. 2, 3, 4 and 5 to predict near-bed load caused by shipping manoeuvres. However, the German and the Dutch approaches apply different coefficients (Table 1).

In the centre of the mixing layer downstream of sills the turbulence energy ($k_{m\ell}$) is

$$k_{m\ell} = \alpha_{k,m\ell} U_s^2 \tag{6}$$

where U_s is the depth-averaged flow velocity above the sill and $\alpha_{k,m\ell}$ is a coefficient.

Turbulence intensities can be expressed by a depth-averaged relative turbulence intensity (r_0), a local relative turbulence intensity (r_u) or a local turbulence energy (k), which are defined as

$$r_0 = \frac{\sqrt{k_0}}{U_0} \tag{7}$$

$$r_u = \frac{u_{\mathrm{RMS}}}{\bar{u}} \tag{8}$$

$$k = \tfrac{1}{2}\left(u_{\mathrm{RMS}}^2 + v_{\mathrm{RMS}}^2 + w_{\mathrm{RMS}}^2\right) \tag{9}$$

where k_0 is the depth-averaged turbulence energy, $\bar{u}$ is the local mean flow velocity in the x direction, U_0 is the depth-averaged flow velocity and u_{RMS}, v_{RMS} and w_{RMS} are the root mean square values of the fluctuating flow velocities in the x, y, and z directions.

For uniform flow conditions Nezu and Nakagawa (1993) found $v_{\mathrm{RMS}} = 0.71 u_{\mathrm{RMS}}$ and $w_{\mathrm{RMS}} = 0.55 u_{\mathrm{RMS}}$. Substituting these empirical relations in Eq. 9 yields $u_{\mathrm{RMS}} \approx k^{0.5}$ and thus $k_{m\ell}$ can be given by

$$k_{m\ell} = \left(r_{u,m\ell}\bar{u}_m\right)^2 \tag{10}$$

where $r_{u,m\ell}$ is the turbulence intensity in the centre of the mixing layer. As given by Van Mierlo and De Ruiter (1988) the maximum value of $\alpha_{k,m\ell}$ is 0.07 for a flow above an artificial dune. Since $U_s \approx \bar{u}_m$ it follows from Eqs. 6 and 10 that the maximum value of $r_{u,m\ell}$ is about 0.26. According to Verheij (1983, 1985) the maximum value of $r_{u,m\ell}$ in a mixing layer of a free jet equals also 0.26. However, the maximum value of $r_{u,m\ell}$ in a mixing layer of a propeller is higher and measures approximately 0.3 (Fig. 3).

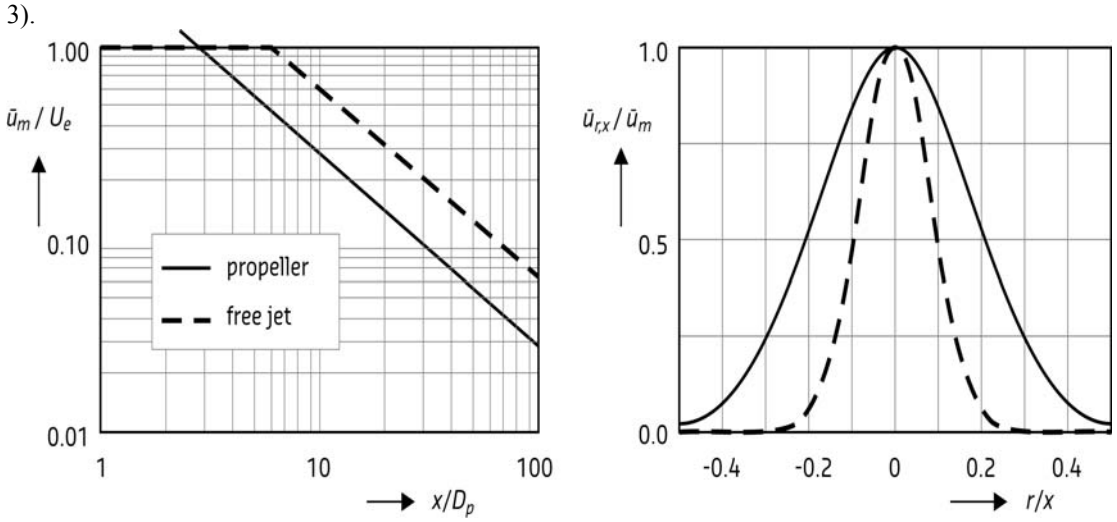

Fig. 2 Differences in flow velocities between propeller and free jets (Verheij 1983, 1985)

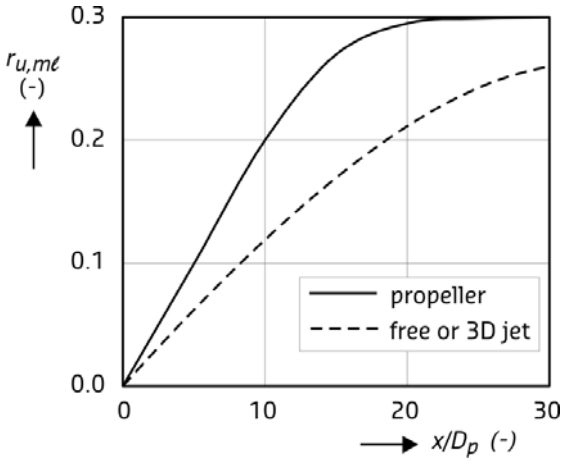

Fig. 3 Differences in turbulence intensities between propeller and free jets (Verheij 1983, 1985)

Assuming that $r_0 = r_{u,m\ell}$ and $U_0 = \bar{u}_{b,m\ell}$ the strength or the erosion resistance of the bed protection must fulfil (see also Hoffmans 2010)

$$\Delta d = 0.7\frac{\left(r_{u,m\ell}\bar{u}_{b,m}\right)^2}{g\Psi_c} \tag{11}$$

where d (= d_{50}) is the mean particle diameter, g is the acceleration due to gravity, Δ (= $\rho_s/\rho - 1$) is the relative density, ρ_s is the density of sediment and Ψ_c is the critical Shields parameter (Shields 1936). When some erosion may occur, that is when $\Psi_c = 0.05$, Eq. 11 can be rewritten with $r_{u,ml} = 0.3$ as

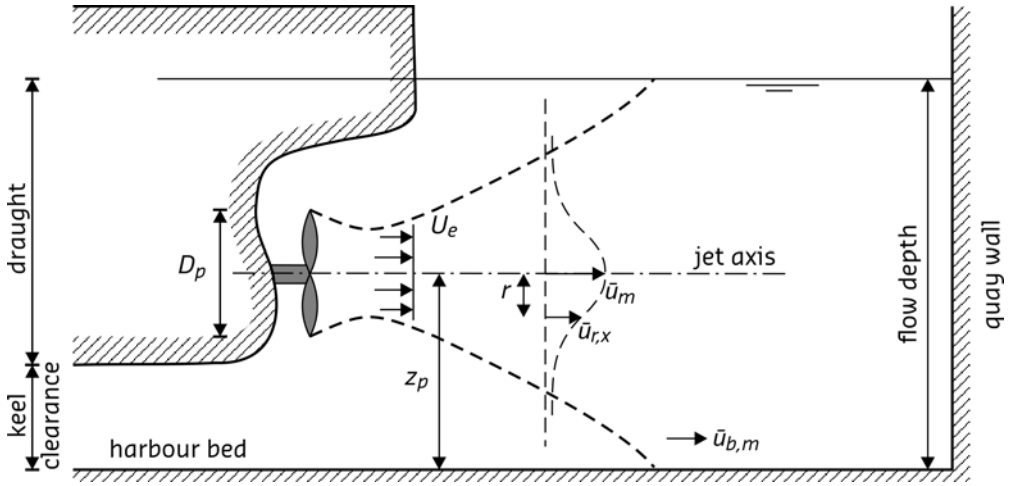

Fig. 4 Flow field behind a free propeller

Table 1 Overview of 3D jet parameters in Eqs. 1, 2, 3, 4 and 5

Parameter	Albertsen et al. 1948[1]	Dutch approach[2]	German approach[3]
α_1	0.081	0.18	0.19 unobstructed jets with $\alpha_2 = 1.0$ 0.27exp[0.092(h/D_p)] without central rudder 0.27exp[0.161(z_p/D_p)] with central rudder 0.56 twin propeller
α_2	1	1	0.25 twin propeller 0.30 extra influence for lateral quay wall 0.60 influence of bed and water surface 1.62 for jets reflected by a quay wall
α_3	0.1 to 0.25 (Rajaratnam, 1976)	0.2[4]	0.25 inland vessels with a tunnel stern and a twin rudder configuration 0.42 sea borne vessels without rudder 0.71 sea borne vessels with rudder

[1] free jet, [2] propeller jet according to Blaauw and Van de Kaa (1978) and Verheij (1983)

[3] propeller jet according to Fueher *et al*. (1981), [4] using $x_r/z_p \approx 6$

$$\Delta d = 2.5 \frac{\overline{u}_{b,m}^2}{2g} \tag{12}$$

resulting in the need for large stones and thus an expensive bed protection. As an alternative mattresses can be applied.

3 Time-dependent scour

Usually propeller load is not continuously at one specific location. Therefore scour as function of time is discussed. From experiments on different scales and with different bed materials scour equations are derived between the time scale and the scales for velocity, turbulence, flow depth and material density. Based on the Dutch systematic research into scour, the shape of the scour hole is independent of bed material and flow velocity. In the development phase the scour as function of time is (e.g. Hoffmans and Verheij 1997)

$$\frac{z_m}{\lambda} = -\left(\frac{t}{t_1}\right)^{\gamma_t} \quad \text{with} \quad t_1 = \frac{K_{330}\lambda^2\Delta^{1.7}}{\left(\alpha U_0 - U_c\right)^{4.3}} \tag{13}$$

where K_{330} [330 hours $m^{2.3}/s^{4.3}$] is a dimensional coefficient, t [hours] is the time, t_1 [hours] is the characteristic time at which $z_m = \lambda$, U_c is the critical depth-averaged flow velocity, U_0 is the depth-averaged flow velocity upstream of the scour hole, z_m is the maximum scour depth as function of time, α (= 1.5 + $5r_0$) is a turbulence coefficient, γ_t is a coefficient representing the type of flow (for 2D → γ_t = 0.4 and for 3D → γ_t = 0.8) and λ is a characteristic length scale.

Verheij (1985) investigated bed stability and scour in harbours caused by propellers. Figure 5 shows the time-dependent scour process for different series in which various hydraulic parameters were varied (d_{50} = 0.0056 m, 0.14 m < h < 0.37 m where h is the flow depth, 0.6 m/s < $\bar{u}_{b,m}$ < 1.0 m/s, 1.5 m/s < U_e < 1.65 m/s and 0.06 m < z_p < 0.16 m).

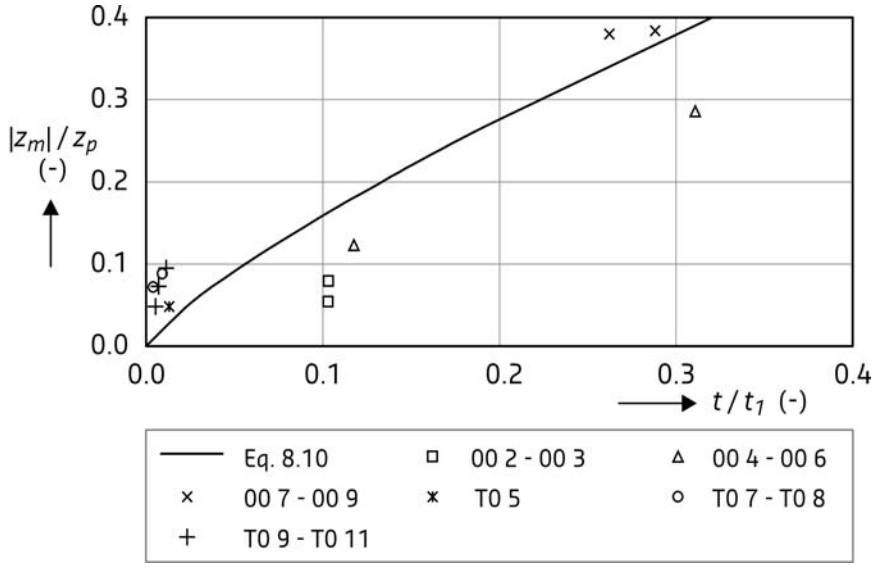

Fig. 5 Time-dependent scour, Experimental data from Verheij (1985); to compute t_1 in Eq. 13 the following assumptions are made: U_c = 0.5 m/s, $U_0 = \bar{u}_{b,m}$, r_0 = 0.2, γ_t = 0.8 and $\lambda = z_p$

4 Two- and three-dimensional horizontal equilibrium scour

For a long time the prediction of the localized scour geometry resulting from 2D-H and 3D-H flow has been an element of the culvert design process for determining erosion protection. Unprotected culvert outlets can induce substantial scouring which may lead to undermining of the culvert. Several researchers have investigated scour caused by submerged horizontal jets over an erodible bed without bed protection (e.g. Hoffmans and Verheij 1997).

The momentum equation is a statement of Newton's law and relates the sum of the forces acting on a control volume per unit width to its rate of change of momentum. In the equilibrium phase of the scour process the sum of forces equals zero. Figure 6 shows a control volume that is representative for the 2D-H as well as the 3D-H scour process. The momentum fluxes and the forces acting on this control volume are the momentum flux (M_1) at the inflow section (section 1)

$$\text{for 2D-H:} \qquad M_1 = \rho q U_1 \tag{14}$$

$$\text{for 3D-H:} \qquad M_1 = \rho Q U_1 \tag{15}$$

where U_1 is the mean jet velocity, q is the discharge per unit width and Q is the total discharge, the momentum flux M_2 at the outflow section (section 2)

$$\text{for 2D-H:} \qquad M_2 = \rho q U_2 \tag{16}$$

$$\text{for 3D-H:} \qquad M_2 = \rho Q U_2 \tag{17}$$

in which U_2 is the mean flow velocity at section 2, the hydrostatic forces (F_1 and F_2), the weight of water (G), the resultant or dynamic force R exerted by the jet on the bed of the scour hole and the angle δ between R and the horizontal. By applying Newton's second law to a control volume in the horizontal direction, the maximum scour depth in the equilibrium phase ($z_{m,e}$) caused by 2D and 3D flow can be written as

$$\text{for 2D-H:} \qquad F_1 - F_2 - R\cos\delta + \rho q\left(U_1 - U_2\right) = 0 \tag{18}$$

$$\text{for 3D-H:} \qquad F_1 - F_2 - R\cos\delta + \rho Q\left(U_1 - U_2\right) = 0 \tag{19}$$

This analysis results in one equation with two unknowns (R and δ) for both 2D and 3D geometries. In principle, the momentum equations can be solved if only one assumption is made for the unknown parameters, which must also be correlated to $z_{m,e}$. The latter correlation allows prediction of the scour hole dimensions.

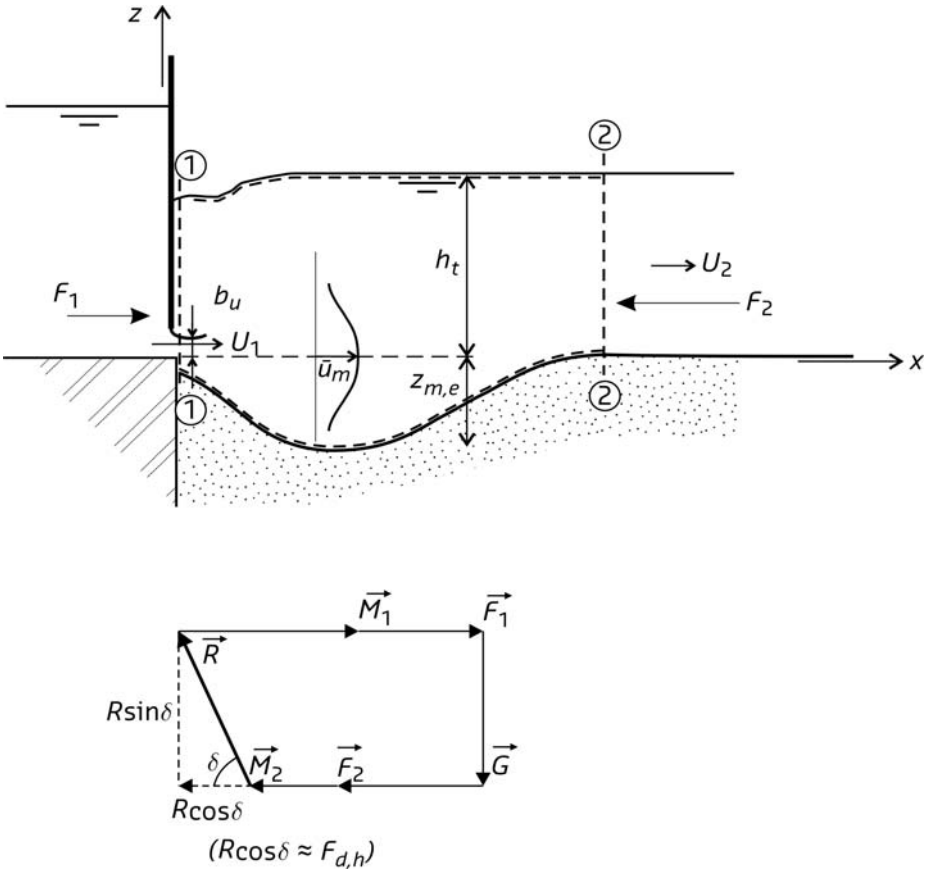

Fig. 6 Definition sketch of jet scour

In general, the weight of water (G) may be written as

$$\text{for 2D-H:} \qquad G = \rho g A \tag{20}$$

$$\text{for 3D-H:} \qquad G = \rho g V \tag{21}$$

in which A is 2D area of control surface shown in Fig. 6 and V is the volume of the control volume. A and G are proportional to the equilibrium scour depth and the tailwater depth (h_t) as

$$\text{for 2D-H:} \qquad A \equiv z_{m,e}\left(z_{m,e} + h_t\right) \tag{22}$$

$$\text{for 3D-H:} \qquad V \equiv z_{m,e}^2\left(z_{m,e} + h_t\right) \tag{23}$$

The unknown $\tan\delta$ is the ratio between the vertical and horizontal resultant force, which for uniform flow can be quantified by first considering the ratio between the friction force (W) and the normal force (N)

$$\frac{W}{N} = \frac{\rho g R_h S_e \ell}{\rho g R_h \ell} = S_e = \tan\phi \tag{24}$$

in which $\tan\phi$ is a friction factor and ϕ is the angle of internal friction, ℓ is the length over which W is acting, R_h is the hydraulic radius and S_e is the mean energy slope. If the mean bed shear stress (τ_0) is larger than the critical mean bed shear stress (τ_c) the dimensions of the scour hole will increase. An equilibrium phase of the maximum scour depth is achieved if $\tau_0 = \tau_c = \rho g R_h S_c$. Using the Shields criterion $\tau_c = \Psi_c(\rho_s - \rho)gd$, the critical mean energy slope is $S_c = \Psi_c \Delta d / R_h$. Assuming that R_h is constant, the inverse of $(\tan\delta)_c$ is proportional to

$$\left(\tan\delta\right)_c^{-1} = \left(\tan\phi\right)_c \equiv \Psi_c \Delta D_{90*} \quad \text{with} \quad D_{90*} = d_{90}\left(\Delta g / \nu^2\right)^{1/3} \tag{25}$$

where D_{90*} is a dimensionless particle, $(\tan\phi)_c$ is the critical friction factor that represents the strength characteristics of loose material and ν is the kinematic viscosity. If both Δ and d increase $(\tan\phi)_c$ also increases in agreement with observations, since the dimensions of a scour hole are relatively larger for lighter and smaller material. Assuming that $h_t << z_{m,e}$ the critical external force reads for 2D-H and for 3D-H respectively

$$\text{for 2D-H:} \qquad \left(R\cos\delta\right)_c = \left(R\sin\delta\left(\tan\delta\right)^{-1}\right)_c = \left(G\tan\phi\right)_c \equiv \rho g z_{m,e}^2 \Psi_c \Delta D_{90*} \tag{26}$$

$$\text{for 3D-H:} \qquad \left(R\cos\delta\right)_c = \left(R\sin\delta\left(\tan\delta\right)^{-1}\right)_c = \left(G\tan\phi\right)_c \equiv \rho g z_{m,e}^3 \Psi_c \Delta D_{90*} \tag{27}$$

If $F_1 = F_2$, $z_{m,e}$ is written as

$$\text{for 2D-H:} \qquad z_{m,e} = c_{2H}\left(q\left(U_1 - U_2\right)/g\right)^{1/2} \quad \text{with} \quad c_{2H} = 20\left(D_{90*}\right)^{-1/2} \tag{28}$$

$$\text{for 3D-H:} \qquad z_{m,e} = c_{3H}\left(Q\left(U_1 - U_2\right)/g\right)^{1/3} \quad \text{with} \quad c_{3H} = 7\left(D_{90*}\right)^{-1/3} \tag{29}$$

in which c_{2H} and c_{3H} are parameters including several uncertainties, e.g. the influence of the tailwater depth, the relative density, the critical Shields parameter, the grading of the bed material and the time duration of the experiments.

Blaisdell and Anderson (1989) investigated scour at cantilevered pipe spillway outlets which are usually used at farm-pond and upstream flood-control principal spillways. About 50 long lasting tests of 165 hours were conducted in which d, D_p (diameter of pipe), U_1, and z_h (height of pipe above tailwater depth) were varied: 2.6 cm < D_p < 81 cm, 0.3 m/s < U_1 < 3.2 m/s and 1 < z_h/D_p < 8. Six different types of sand were used in which d_{50} ranged from 0.46 mm to 7.65 mm. Using Eq. 29 the data of Blaisdell and Anderson (1989) is simulated with an accuracy of 0.5 < ξ < 2, in which ξ is the discrepancy ratio between measured and calculated scour depth.

Martins (1973) analysed scour due to a 3D jet falling on a rocky river-bed. The river bed consisted of equal cubic blocks systematically arranged without cohesion (d_{50} = 3 cm and 4.7 cm). Based on 90 experiments in which h_t, H (is the drop head), Q, and θ (is the angle of impact with the horizontal) were varied (0.06 m < h_t < 0.40 m, 0.9 m < H < 2.1 m, 0.011 m^3/s < Q < 0.0368 m^3/s and 40^o < θ < 70^o), Martins arrived by using Albertson's et al. (1948) theory at

$$z_{m,e} = 0.14 N_M + 0.7 h_t - 0.73 h_t^2 / N_M \quad \text{with} \quad N_M = Q^{3/7} H^{3/14} / d_{50}^{2/7} \tag{30}$$

where N_M [m$^{17/14}$/s$^{6/14}$] is a dimensional coefficient. If h_t equals zero and using $U_1 = (2gH)^{0.5}$, Eq. 30 reduces to

$$z_{m,e} = c_{3M}\left(QU_1 / g\right)^{3/7} \quad \text{with} \quad c_{3M} = 3.6 / D_{50*}^{2/7} \tag{31}$$

whence follows that Eqs. 29 and 31 are almost identical with small differences in the exponents (namely 1/3 and 3/7) and the parameters c_{3H} and c_{3M}.

Other important design parameters with respect to jet scour are the length (L_s) and the width (B_s) of the scour hole. For both circular and plane jets, experiments have indicated that the ratios $L_s/z_{m,e}$ and $B_s/z_{m,e}$ are nearly constant and measure $L_s/z_{m,e} = 7$ and $B_s/z_{m,e} = 2$ (e.g. Breusers and Raudkivi 1991).

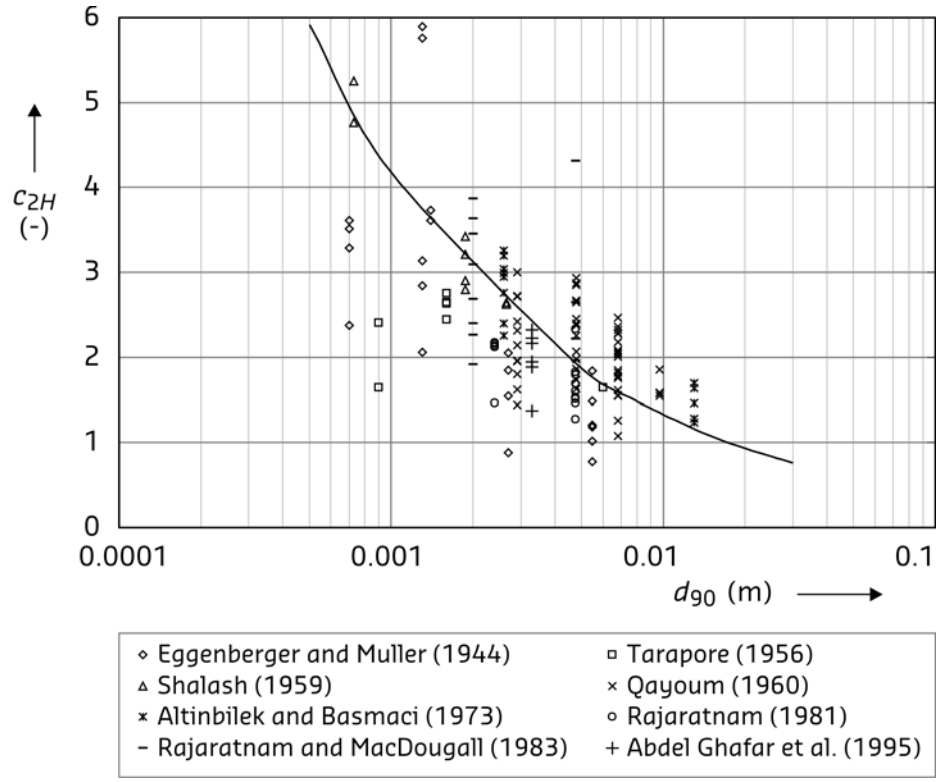

Fig.7 c_{2H} as function of d_{90} (Scour data base; see also Hoffmans 1995)

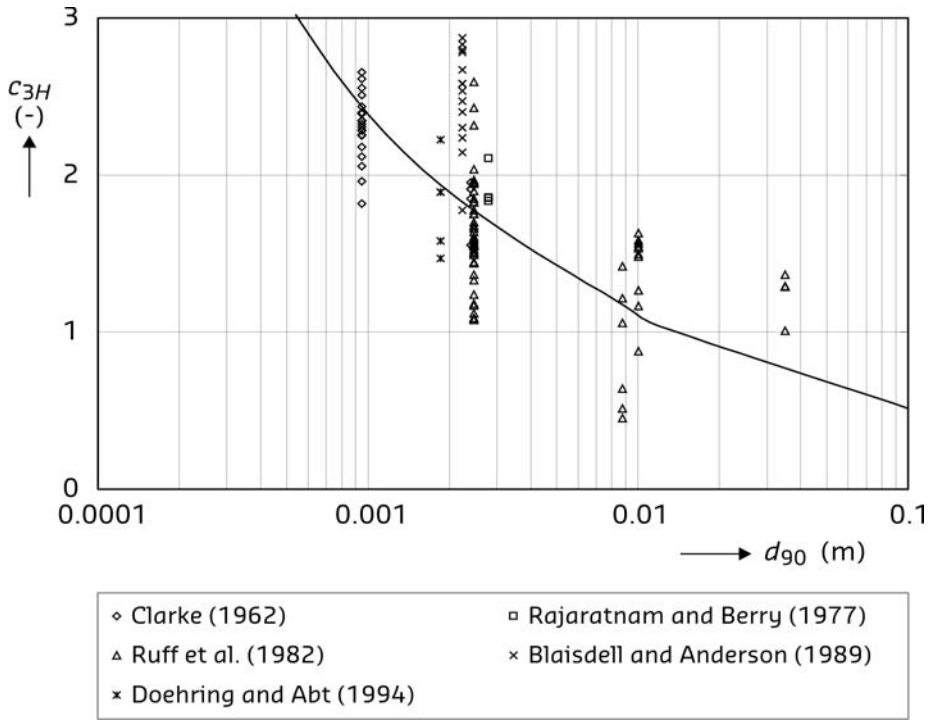

Fig. 8 c_{3H} as function of d_{90} (Scour data base; see also Hoffmans 1995)

The calibration and verification of c_{2H} were based on about 125 experiments in which the test section consisted of non-cohesive material. The hydraulic conditions were nearly identical and no prototype experiments were used. The scour parameter c_{3H} was calibrated and validated by using more than 100 flume tests. Figures 7 and 8 demonstrate that $z_{m,e}$ slightly increases if the particle diameter decreases, which is in agreement with the experimental results in which sand was considered in the range of 1 mm $< d_{90} <$ 40 mm with $g = 9.81$ m/s^2, $\Delta = 1.65$ and $\nu = 10^{-6}$ m^2/s.

The scour database (Hoffmans 1995) that has been used to calibrate and verify Eqs. 28 and 29, contains little information with respect to the duration of the experiments. Usually researchers terminate their tests when the scour rate slows (stabilization phase), not when a stable scour hole is achieved. Part of the relatively large scatter in Figs. 7 and 8 can be ascribed to lack of definition of the equilibrium phase.

For horizontal jets, F_1 is assumed to be equal to F_2, which is a fair assumption only if the flow depth downstream of the hydraulic structure is about equal to the tailwater depth. When the jump is unstable, i.e. when the jump is receding to a point far downstream of the outlet, the assumption $F_1 = F_2$ cannot be used. The large scatter in the results can also be attributed to the unstable form of the jet or the magnitude of the jet velocity. If the jet is not attached, but if a recirculation zone and a mixing layer occur (surface jet), the flow velocities in the scour hole are significantly lower. The different jets in relation to the magnitude of scouring are here not examined. Since no prototype tests were used to verify Eqs. 28 and 29, it is a rather narrow basis for the assumption that the values of the unknowns c_{2H} and c_{3H} are the best values.

Although c_{2H} and c_{3H} are calibrated and validated by using fines, coarse sand and gravel Eqs. 28 and 29 could easily be extended to cohesive soils provided $(\tan\phi)_c$ is related to the erosion resistance parameters, for example the cohesion. To increase the accuracy of the predictions both desk studies and detailed physical model studies will have to be carried out. Newton's second law and new developments in the modelling of coherent structures (e.g. Nezu and Nakagawa, 1993) will help to accomplish this goal.

5 Two-dimensional oblique equilibrium scour

Plunging jets (Fig. 9) are often used to pass excess floodwaters from a dam to a downstream river. Downstream of the dam a scour hole will be formed, which, if extensive, may endanger the stability of the dam itself. Therefore the equilibrium size of the scour hole has to be known at the design stage to ensure the safety of the dam. The extent of scour for a particular design flood is dependent on the interaction between hydraulic and geological factors, a relation that is not always fully appreciated by researchers.

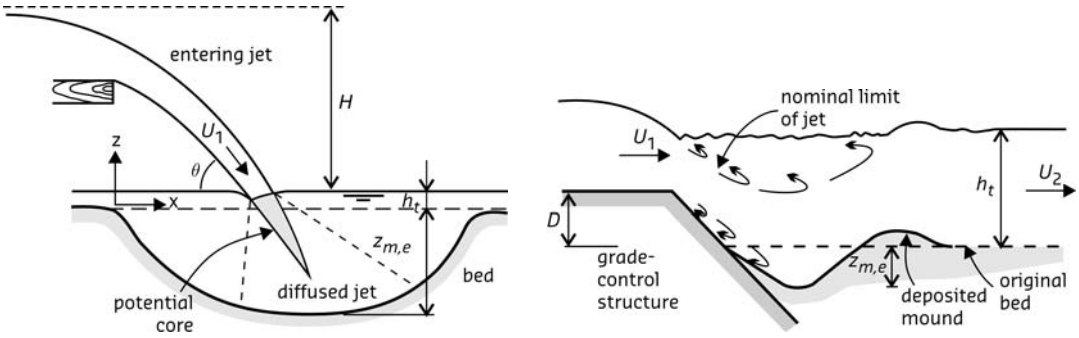

Fig. 9 a) Plunging jets, head cut b) Grade-control structure with D as drop height

Figure 10 shows a control volume that is representative for the scour process downstream of hydraulic structures. Application of Newton's law gives per unit width with θ is the angle of impingement (see also Section 4)

$$-G + R\sin\delta - \rho q U_1 \sin\theta = 0 \tag{32}$$

Based on a set of eight equations and eight unknowns Hoffmans (2009) found

$$z_{m,e} + h_t = \frac{\text{load}}{\text{strength}} = \frac{\sqrt{qU_1 \sin\theta / g}}{\left(c_{2V}\right)^{-1}} \tag{33}$$

with

$$c_{2V} = \sqrt{\frac{20}{D_{90*}^{2/3}}} \tag{34}$$

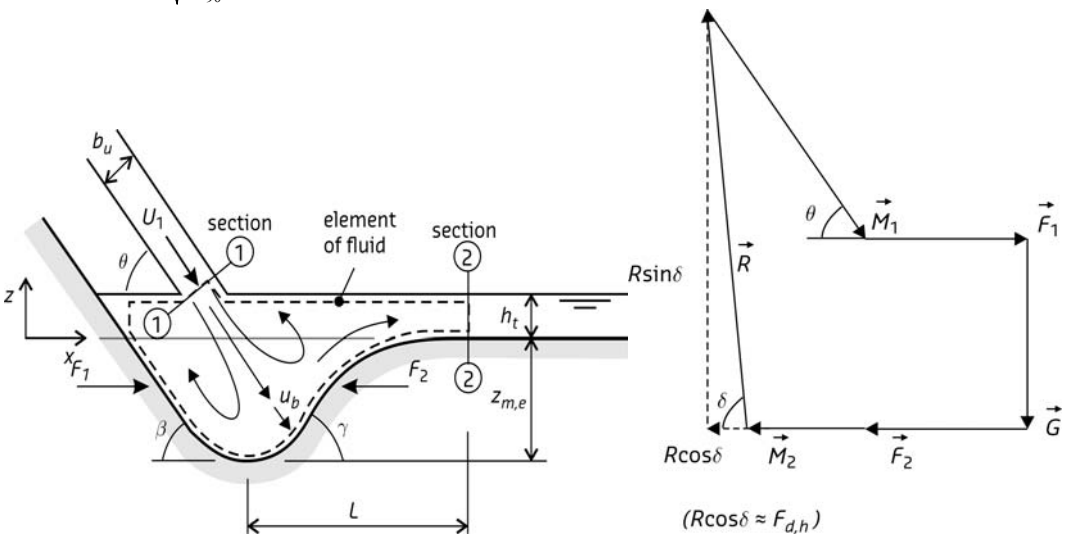

Fig. 10 a) Definition sketch b) Forces

6 Three-dimensional vertical equilibrium scour

Besides 2D horizontal scour Clarke (1962) also studied scour caused by vertical 3D jets with variable parameters U_1 and D_p (2.4 mm < D_p < 14.3 mm) in sand (0.44 mm < d < 2 mm). He observed static as well as dynamic scour. Dynamic scour is larger than static scour because at higher velocities more particles can go into suspension giving a hemispherical scour hole (Fig. 11). The ratio between dynamic scour (z_{sd}) and static scour (z_{ss}) lies in the range of 1.2 to 2.0. Based on Rajaratnam tests with a 3D jet impinging on a sandy bed with 1.2 mm < d_{50} < 2.38 mm, Breusers and Raudkivi (1991) described z_{ss} as

$$z_{ss} = \alpha_{RAJ} D_p U_1 / \sqrt{\Delta g d_{50}} \quad \text{with} \quad \alpha_{RAJ} = 0.3 \tag{35}$$

which is comparable to Eq. 29, since Eqs. 29 and 35 can be rewritten as

$$\text{Eq. 29} \quad z_{m,e} \equiv \left(\left(D_p U_1\right)^2 / d_{90}\right)^{1/3} \quad \text{and} \quad \text{Eq. 35} \quad z_{ss} \equiv \left(\left(D_p U_1\right)^2 / d_{50}\right)^{1/2}$$

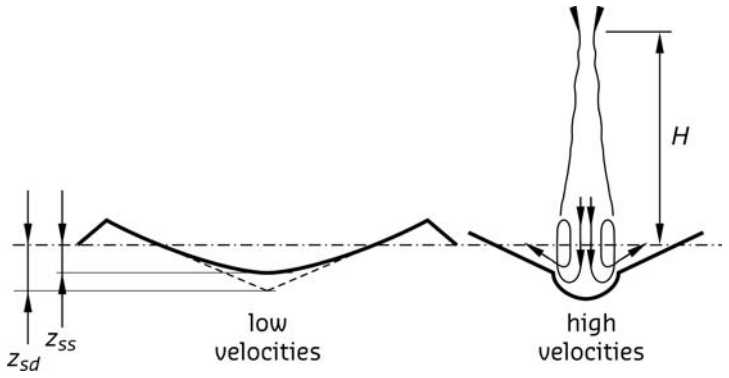

Fig. 11 Static and dynamic scour (Breusers and Raudkivi 1991)

Rajaratnam (1981b) also carried out tests with a low tailwater depth and jet sizes of D_p is 9.8 mm and 12.7 mm in sand beds with d = 1.0, 1.15 and 2.38 mm. Under these conditions Breusers and Raudkivi (1991) reported a lower value for α_{RAJ}, namely α_{RAJ} = 0.13. However, the ratio between z_{ss} and z_{sd} was larger and reached values up in the range 2 to 4.

7 Conclusions

The change in momentum per unit of time in the control volume flowing in a channel is equal to the resultant of all the external forces that are acting on the element. Despite the simplifications made in applying the momentum principle to a control volume representing the equilibrium shape of a scour hole, this study has shown that the method can be used to calculate scour for sand and gravel caused by 2D-H, 3D-H and 2D-V jets within an accuracy of $0.5 < \xi < 2$ where ξ is the ratio between the calculated and measured scour depth.

References

Abdel Ghafar, A., Mossa, M. and Petrillo, A. (1995). Scour from flow downstream of a sluice gate after a horizontal apron, 6th Int. Symp. on River Sedimentation, New Delhi, India, pp.1069-1088.

Albertson, M.L., Dai,Y.B., Jensen R.A., Rouse, H. (1948). Diffusion of submerged jets, ASCE, *Trans. Paper No. 2409*, pp. 639-664.

Altinbilek, H.D. and Basmaci, Y. (1973). Localized scour at the downstream of outlet structures, *Proc. 11th Congress on large dams*, Madrid, pp.105-121.

Blaauw, H. G., Van de Kaa, E. J., 1978. Erosion of bottom and banks caused by the screw race of manoeuvring ships, Publication No. 202, Deltares, Delft.

Blaisdell, F.W. and Anderson, C.L. (1989). Scour at cantilevered outlets: Plunge pool energy dissipator design criteria, ARS-76, U.S. Department of Agriculture, Agricultural Research Service, Washington, D.C.

Breusers, H.N.C. and Raudkivi, A.J. (1991). *Scouring*. IAHR Hydraulic structures design manual 2. Balkema, Rotterdam.

Clarke, F.R.W. (1962). The action of submerged jets on moveable material, *Master Thesis*, Department of Civil Engineering, Imperial College, London.

Doehring, F.K. and Abt, S.R. (1994). Drop height influence on outlet scour, *J. Hydr. Engrg.*, 120(12), pp.1470-1476.

Eggenberger, W. and Müller, R. (1944). Experimentelle und theoretische Untersuchungen über das Kolk-problem, Mitteilungen aus der Versuchsanstalt für Wasserbau, Nr.5, Zurich, Switzerland.

Fuehrer, M., Römisch, K. and Engelke, G. (1981). Criteria for dimensioning the bottom and slope protection and for applying the new methods of protecting navigation canals, *25th Int.Navigation Congr., PIANC*. Section 1, Subject 1, Edinburgh, pp. 29-50.

Hoffmans, G.J.C.M. (1995). Scour due to submerged jets. Report W-DWW-94-303, [in Dutch], Min. of Public Works, Rijkswaterstaat, Delft.

Hoffmans, G.J.C.M. and Verheij, H.J. (1997). *Scour manual*, Balkema, Rotterdam.

Hoffmans, G.J.C.M. (2009). Closure problem to jet scour, *J. Hydr. Res.*, 47(1), pp.100–109.

Hoffmans, G.J.C.M. (2010). Stability of Stones Under Uniform Flow, *J. of Hydr. Engrg.*, *ASCE*, 136(2), pp. 129-136.

Martins, R. (1973). Contribution to the knowledge on the scour action of free jets on rocky river-beds, *Proc. 11th* Congress on Large Dams, pp. 799-814.

Nezu, I. and Nakagawa, H. (1993). *Turbulence in Open-Channel Flows*, IAHR-Monograph, Balkema, Rotterdam.

Qayoum, A. (1960). Die Gesetzmäβigkeit der Kolkbildung hinter unterströmten Wehren unter spezieller Berück-sichtigung der Gestaltung eines beweglichen Sturzbettes, Dissertation, Technischen Hochschule Carolo-Wilhelmina, Braunschweig, Germany.

Rajaratnam, N. (1976). *Turbulent Jets*, Elsevier, Amsterdam.

Rajaratnam, N. (1981). Erosion by plane turbulent jets, *J. Hydr. Res.*, 19(4), pp. 339-358.

Rajaratnam, N. (1981b). Erosion of sand beds by circular impinging jets with minimum tailwater, University of Alberta, Edmonton, Alberta.

Rajaratnam, N. and Berry, B. (1977). Erosion by circular turbulent wall jets, *J. Hydr. Res.*, 15(3), pp. 277-289.

Rajaratnam, N. and MacDougall, R.K., (1983). Erosion by plane wall jets with minimum tailwater, *J. of Hydr. Engrg.*, *ASCE*, 109(7) pp.1061-1064.

Ruff, J.F., Abt, S.R., Mendoza, C., Shaikh, A. and Kloberdanz, R. (1982). Scour at culvert outlets in mixed bed materials, *Report* FHWA/RD-82/011, Colorado State Univ., Fort Collins, Colorado, USA.

Schoklitsch, A. (1935). *Stauraumverlandung und Kolkabwehr,* Verlag von Julius Springer, Vienna, Austria.

Schoklitsch, A. (1962). *Die kolkbildung, Handbuch des Wasserbaues*, Erster Band, pp. 200-210.

Shalash, M.S.E. (1959). Die Kolkbildung beim Ausfluβ unter Schützen, Dissertation, Technischen Hochschule München, Germany.

Shields, A. (1936). Anwendung der Aehnlichkeitsmechanik und der Turbulenzforschung auf die Geschiebe-bewegung, Mitteilungen der Preusischen Versuchsanstalt für Wasserbau und Schiffbau, Heft 26, Berlin NW 87.

Tarapore, Z.S. (1956). Scour below a submerged sluice gate, *Master Thesis*, University of Minnesota, USA.

Van Mierlo, M.C.L.M. and De Ruiter, J.C.C. (1988). Turbulence measurements above dunes, *Report* Q789, Vol. 1 and 2, Deltares, Delft.

Verheij, H.J. (1983). The stability of bottom and banks subjected to the velocities in the propeller jet behind ships, *Publication* No. 303, Deltares, Delft.

Verheij, H.J. (1985). Propeller jets and bed stability [in Dutch], *Report* M1115 parts VI and Xa, Deltares, Delft.